Quartz Crystal Microbalance (QCM) in High-Pressure Carbon Dioxide (CO₂): Experimental Aspects of QCM Theory and CO₂ Adsorption

You-Ting Wu,[†] Paa-Joe Akoto-Ampaw,[†,§] Mohamed Elbaccouch,[†,‖]
Michael L. Hurrey,[‡] Scott L. Wallen,[‡] and Christine S. Grant*,[†]

*Department of Chemical Engineering, Box 7905, North Carolina State University,
Raleigh, North Carolina 27695-7905, and Department of Chemistry, CB# 3290,
Kenan and Venable Laboratories, The University of North Carolina,
Chapel Hill, North Carolina 27599-3290*

The quartz crystal microbalance (QCM) technique has been developed into a powerful tool for the study of solid−fluid interfaces. This study focuses on the applications of QCM in high-pressure carbon dioxide (CO₂) systems. Frequency responses of six QCM crystals with different electrode materials (silver or gold) and roughness values were determined in helium, nitrogen, and carbon dioxide at 35−40 °C and at elevated pressures up to 3200 psi. The goal is to experimentally examine the applicability of the traditional QCM theory in high-pressure systems and determine the adsorption of CO₂ on the metal surfaces. A new QCM calculation approach was formulated to consider the surface roughness contribution to the frequency shift. It was found that the frequency−roughness correlation factor, C_r, in the new model was critical to the accurate calculation of mass changes on the crystal surface. Experiments and calculations demonstrated that the adsorption (or condensation) of gaseous and supercritical CO₂ onto the silver and gold surfaces was as high as 3.6 μg cm^{-2} at 40 °C when the CO₂ densities are lower than 0.85 g cm^{-3}. The utilization of QCM crystals with different roughness in determining the adsorption of CO₂ is also discussed.

1. Introduction

In the past few years, there has been increased interest in the application of the piezoelectric quartz crystal microbalance (QCM) for the study of solid−fluid interfaces.[1−4] The high mass sensitivity (ng cm^{-2}) of the QCM has been especially useful for the investigation of surface films: (1) for adsorption, absorption, deposition, and dissolution;[1,5] (2) for molecular recognition;[3,6] (3) for anion adsorption;[1] and (4) for many other chemical processes.[1,3,4] The advantages of conceptual simplicity, miniature and rigid size, relative ease of surface modification, chemical inertness of the quartz substrates, and low cost have encouraged the development of various sensor applications.[2,3] In particular, the QCM, as a piezoelectric device, has very few limitations for microweighing in extreme pressure environments (i.e., supercritical CO₂). The extreme pressure environments usually exclude the use of other conventional microbalances, such as spring, beam, and torsional balances, due to the difficulties associated with the transfer of gravimetric forces from the sample to the balance under such extreme conditions.[7]

Supercritical and liquid CO₂ have received increasing

industrial and research attention[8,9] due to their advantages over conventional organic solvents (i.e., chlorofluorocarbons). These advantages include the tunable dissolving power with temperature and pressure, low viscosity, high diffusivity, low cost, modest critical temperature and pressure (31 °C and 1070 psi), and especially the environmentally benign features (e.g., nontoxic, nonflammable, and minimal environmental impact). CO₂ has been most widely used as a solvent in extraction, cleaning, and dissolution applications.[10−12] In all these applications, the real-time monitoring of the rate of dissolution, cleaning, or extraction and the determination of other chemical and physical properties (i.e., solubility) associated with these processes are very important. This monitoring or determination is a great challenge due to the lack of various detection methods under extreme conditions. The purpose of the current research is to extend the use of QCM to high-pressure CO₂-based environments.

The QCM microweighing technique utilizes the linear relationship between the frequency shift and the mass change observed on the QCM surface. This basic correlation, known well as the Sauerbrey equation,[13] was originally used in a vacuum.[5] However, the QCM frequency in a high-pressure fluid is affected by the pressure, viscosity, and density of the surrounding fluid, as well as the adsorbed mass on the crystal surface. Urbakh and co-workers[14,15] further pointed out that the theory gov-

* Corresponding author.

† North Carolina State University.

‡ The University of North Carolina.

§ Current address: Shell Exploration & Production Company, 200 N. Dairy Ashford Rd., Houston, TX 77079.

‖ Current address: Florida Solar Energy Center, 1679 Clearlake Road, Cocoa, FL 32922.

(1) Buttry, D. A.; Ward, M. D. *Chem. Rev.* **1992**, *92* (6), 1355−1379.
(2) Ward, M. D.; Buttry, D. A. *Science* **1990**, *249* (4972), 1000−1007.
(3) O'Sullivan, C. K.; Guilbault, G. G. *Biosens. Bioelectron.* **1999**, *14* (8−9), 663−670.
(4) Thompson, M.; Kipling, A. L.; Duncanhewitt, W. C.; Rajakovic, L. V.; Cavicvlasak, B. A. *Analyst* **1991**, *116* (9), 881−890.
(5) Lu, C.; Czanderna, A. W. *Applications of piezoelectric quartz crystal microbalances*; Methods and phenomena, their applications in science and technology, Vol. 7; Elsevier: New York, 1984.
(6) Wegener, J.; Janshoff, A.; Steinem, C. *Cell Biochem. Biophys.* **2001**, *34* (1), 121−151.
(7) Sato, Y.; Takikawa, T.; Takishima, S.; Masuoka, H. *J. Supercrit. Fluids* **2001**, *19* (2), 187−198.

(8) DeSimone, J. M. *Science* **2002**, *297* (5582), 799−803.
(9) McCoy, M. *Chem. Eng. News* **1999**, *77* (24), 11−13.
(10) McHardy, J.; Sawan, S. P. *Supercritical fluid cleaning: Fundamentals, technology, and applications*; Noyes Publications: Westwood, NJ, 1998.
(11) Mchugh, M. A.; Krukonis, V. J. *Supercritical fluid extraction: principles and practice,* 2nd ed.; Butterworth-Heinemann: Stoneham, U.K., 1993.
(12) Sundararajan, N.; Yang, S.; Ogino, K.; Valiyaveettil, S.; Wang, J. G.; Zhou, X. Y.; Ober, C. K.; Obendorf, S. K.; Allen, R. D. *Chem. Mater.* **2000**, *12* (1), 41−48.
(13) Sauerbrey, G. *Z. Phys.* **1959**, *155* (2), 206−222.
(14) Urbakh, M.; Daikhin, L. *Langmuir* **1994**, *10* (8), 2836−2841.
(15) Urbakh, M.; Daikhin, L. *Phys. Rev. B* **1994**, *49* (7), 4866−4870.

erning QCM frequency response in a fluid is yet highly undeveloped due to the microscopic properties of interfaces and the associated surface roughness. Therefore, it becomes extremely important to separate out each influencing factor, in order to calculate the actual absorbed/deposited mass on the crystal surface. In addition, the investigation of CO_2 adsorption on blank QCM crystals is a required initial step for the successful use of the QCM technique to investigate chemical and physical properties of surface films (coated on the QCM surface) in CO_2. This paper will focus on an experimental examination of the QCM theory and the adsorption of CO_2 on metal surfaces.

In the literature, there have been a limited number of QCM applications in high-pressure CO_2. More fundamental research is required to fully elucidate the QCM behavior in CO_2. Otake et al.[16] determined the mass of CO_2 adsorbed onto rough silver surfaces of QCM at 40 °C and at pressures up to 5800 psi. Guigard and co-workers[17] evaluated the adsorption of CO_2 on rough gold electrodes and extended the use of QCM to determine the solubility of bis(acetylacetonato) copper and bis(thenoyltrifluoro-acetonato) copper (coated on gold electrodes) in super-critical CO_2 at 40−45 °C and pressures up to 1500 psi. The adsorption and solubility (e.g., absorption) of CO_2 to polystyrene have been carried out on a gold QCM surface at 40 °C and pressures up to 2500 psi.[18] The solubility of CO_2 in a variety of polymers such as polycarbonate and Teflon at pressures up to 1500 psi has been reported.[19] The most recent reported use of the QCM technique in CO_2 is the biological work by Okahata's research group. They used the QCM to investigate the molecular recognition of nucleobases with thymine and an organic crystal with ethyl acetate in supercritical CO_2 at 1450 psi and 40 °C.[20,21] All these efforts have portended the broad development of QCM applications in CO_2. However, none of the research mentioned above have taken into account the contribution of surface roughness (microscopic properties of the interface) to the QCM frequency response, which was used to calculate the mass loading. To date, there is still a lack of a comprehensive examination of the QCM theory in high-pressure CO_2 systems.

This paper presents an evaluation of the frequency response of six QCM crystals which have varying surface roughness and different electrode materials (silver and gold) in three fluids, He, N_2, and CO_2, at 35−40 °C and pressures up to 3200 psi. The goal is to separate out all frequency-influencing factors, examine the QCM theory in high-pressure CO_2, and calculate the amount of CO_2 adsorbed on metal surfaces.

2. QCM Theory in High-Pressure Fluids

2.1. Basic Fundamentals. A mechanical stress applied to the surfaces of quartz crystals can afford a corresponding electrical potential across the crystal.[2] This behavior is referred to as the piezoelectric effect. Conversely, application of an alternating electric field across the thickness of an AT-cut quartz crystal by two excitation electrodes on opposite sides of the crystal results in shear

vibration. The shear motion induces an acoustic wave that propagates through the crystal in the thickness direction. A resonant oscillation with a standing wave is achieved when the crystal is driven by the electric field at a frequency matching the fundamental frequency of the crystal (F_0).

When the crystal is immersed in a high-pressure fluid, any shift of frequency from its fundamental value (F_0) in a vacuum can be observed due to contributions from (1) the mass of foreign layers deposited on the crystal surface, (2) the pressure, (3) the density and viscosity of the fluid surrounding the crystal, and (4) the surface roughness of the crystal. The following expression has been established to describe the frequency shift, ΔF, due to the aforementioned effects:[22]

$$\Delta F = F - F_0 = \Delta F_m + \Delta F_P + \Delta F_\eta + \Delta F_r \quad (1)$$

where F is the measured frequency of quartz, ΔF_m relates to mass loading, ΔF_P is dependent on pressure, ΔF_η changes with density and viscosity, and ΔF_r is a function of surface roughness.

The frequency change of a crystal due to the mass loading, ΔF_m, is the fundamental principle of operation of QCMs. According to the well-known Sauerbrey equation,[13] ΔF_m is directly proportional to the mass change on the crystal as given by

$$\Delta F_m = -2nF_0^2 \Delta m/(\mu_q \rho_q)^{1/2} = -C_m \Delta m \quad (2)$$

where $\mu_q = 2.947 \times 10^{11}$ g cm^{-1} s^{-2} is the shear modulus of quartz, $\rho_q = 2.648$ g cm^{-3} is the density of the crystal, Δm is the change of mass per real surface area (g cm^{-2}), and n (=1 or 2) is the number of faces of the crystal in contact with the fluid. Under high pressure, both faces should be exposed to the fluid to prevent breakage. C_m is the mass sensitivity of the QCM and is a function of the characteristic properties (F_0, μ_q, and ρ_q) of the quartz crystal. Equation 2 applies only if the mass of the foreign material is much less than the mass of the crystal, and it assumes that this mass is firmly attached to the surface, and hence the foreign material moves together with the crystal. Such conditions are usually assumed to be fulfilled in cases of rigid layers of coated solid films and self-assembled monolayers.[1,5]

The pressure dependence of frequency, ΔF_P, increases linearly with increasing pressure, as shown by Stock-bridge[23] for gases up to 15 psi. Susse[24] described a similar relationship for liquids up to 1.5×10^4 psi. Thus, ΔF_P can be written as

$$\Delta F_P = F_0 \alpha P = C_P P \quad (3)$$

where α is the proportionality constant and C_p is the pressure sensitivity of the QCM crystal, both of which are independent of the type of fluid in contact with the crystal. C_P is calculated to be 0.36 for a 5 MHz crystal from the value of α proposed by Stockbridge when pressure (P) is expressed in psi.

The viscosity and density contribution, ΔF_η, describes the interaction of the vibrating crystal with a Newtonian viscous fluid. This interaction leads to an additional loading of the crystal, causing a decrease in frequency. ΔF_η is expressed to be proportional to the square root of

(16) Otake, K.; Kurosawa, S.; Sako, T.; Sugeta, T.; Hongo, M.; Sato, M. *J. Supercrit. Fluids* **1994**, *7* (4), 289−292.

(17) Guigard, S. E.; Hayward, G. L.; Zytner, R. G.; Stiver, W. H. *Fluid Phase Equilib.* **2001**, *187*, 233−246.

(18) Miura, K.; Otake, K.; Kurosawa, S.; Sako, T.; Sugeta, T.; Nakane, T.; Sato, M.; Tsuji, T.; Hiaki, T.; Hongo, M. *Fluid Phase Equilib.* **1998**, *144* (1−2), 181−189.

(19) Aubert, J. H. *J. Supercrit. Fluids* **1998**, *11* (3), 163−172.

(20) Mori, T.; Naito, M.; Irimoto, Y.; Okahata, Y. *Chem. Commun.* **2000**, (1), 45−46.

(21) Naito, M.; Sasaki, Y.; Dewa, T.; Aoyama, Y.; Okahata, Y. *J. Am. Chem. Soc.* **2001**, *123* (44), 11037−11041.

(22) Tsionsky, V.; Daikhin, L.; Urbakh, M.; Gileadi, E. *Langmuir* **1995**, *11* (2), 674−678.

(23) Stockbridge, C. D. Effects of gas pressure on quartz crystal microbalances. In *Vacuum Microbalance Techniques*; Behrndt, K. H., Ed.; Plenum Press: New York, 1966; p 147.

(24) Susse, C. *J. Phys. Radium* **1955**, *16* (4), 348−349.
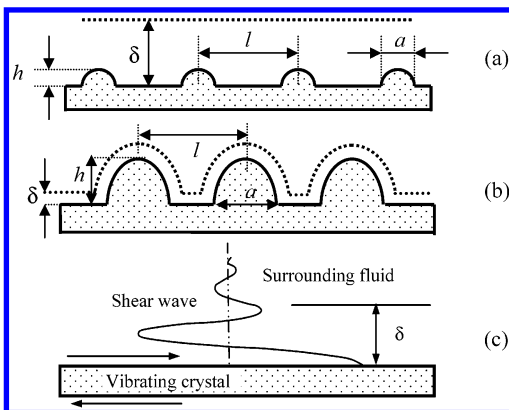
Figure 1. Schematic views of the surface roughness of crystals and the decay length of fluid velocities: (a) slightly rough surface, $h/\delta \ll 1$; (b) strongly rough surface, $h/\delta \gg 1$; (c) decay length, δ, an effective thickness of the surrounding fluid that is driven to move by the vibrating crystal.

the product of viscosity and density of the surrounding fluid:[23,25]

$$\Delta F_\eta = -0.5 C_m (\pi F_0)^{-1/2} (\rho_f \eta_f)^{1/2} \qquad (4)$$

where ρ_f and η_f are the absolute density and viscosity of the bulk fluid, respectively.

2.2. Roughness Effect. A common feature of the approaches to QCM theory as reviewed by Thompson et al.[4] is to neglect the microscopic properties of interfaces and surface roughness.[14] This leads to deviations of most experimental frequency shift data from the predictions by these approaches. Buttry and Ward[1] and Schumacher et al.[26] observed that up to 80% of the observed frequency shifts for a crystal in contact with a liquid under atmospheric pressure and temperature conditions could be attributed to roughness effects.

Since the microscopic properties of crystal–fluid interfaces change with the real surface morphology, a predictive analytical expression for the roughness contribution to frequency, ΔF_r, is not available. However, Urbakh et al.[14,15,27] formulated an ideal model for surface roughness, assuming that a rough surface can be characterized by the average height (h), lateral length (a), and distance (l) between the inhomogeneities of the surface (Figure 1). They incorporated this model into a perturbation theory framework[14,15] and derived a general relationship for ΔF_r as

$$\Delta F_r = -0.5 C_m (\pi F_0)^{-1/2} (\rho_f \eta_f)^{1/2} \Psi(a/\delta, a/l, h/a) \qquad (5)$$

where Ψ is a scaling function, related to three dimensionless factors, a/δ, a/L, and h/a; δ is the decay length of fluid velocities, an effective thickness of the fluid that is driven to move by the vibrating crystal with a displacement decaying exponentially (see Figure 1). This length varies with ρ_f, η_f, and F_0 and is expressed as

$$\delta = [\eta_f/(\pi F_0 \rho_f)]^{1/2} \qquad (6)$$

The value of δ is calculated to be on the order of $0.1-1 \times 10^{-4}$ cm for all gases (i.e., He, N₂, and gaseous CO₂) in this study and $0.07-0.11 \times 10^{-4}$ cm for supercritical CO₂.

(25) Kanazawa, K. K.; Gordon, J. G., II *Anal. Chim. Acta* **1985**, *175*, 99–105.
(26) Schumacher, R.; Borges, G.; Kanazawa, K. K. *Surf. Sci.* **1985**, *163* (1), L621–L626.
(27) Daikhin, L.; Urbakh, M. *Langmuir* **1996**, *12* (26), 6354–6360.
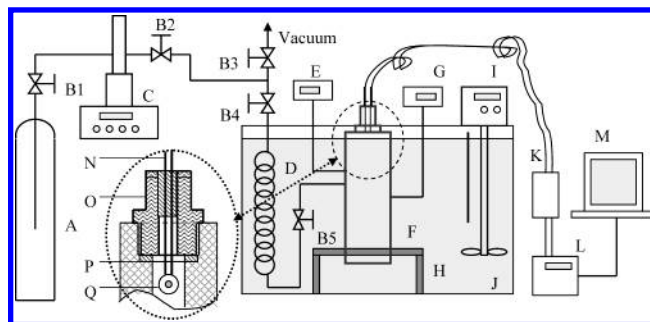
Figure 2. Schematic diagram of the pressure cell and apparatus. (A) CO₂ cylinder; (B1–B5) valves; (C) ISCO pump; (D) preheating coil; (E) pressure transducer; (F) pressure cell; (G) thermocouple and temperature indicator; (H) stand; (I) circulator and heater for water bath; (J) water bath; (K) oscillator circuit; (L) frequency counter; (M) computer; (N) feedthrough leads; (O) feedthrough; (P) O-ring; (Q) quartz crystal.

In particular, if one assumes a slowly varying roughness ($h/a \ll 1$ and $h/\delta \ll 1$) for the crystal surface with limits of $a/\delta \ll 1$ or $a/\delta \gg 1$, the scaling function Ψ is proportional to the ratio a/δ.[14] Reformulating eq 5 yields

$$\Delta F_r = -0.5 C_m C_r \rho_f \qquad (7)$$

where $C_r = \Psi \delta$ is defined as the frequency–roughness correlation factor. This factor is only a function of surface roughness (h, l, and a), provided that the assumptions above are fully established. Equation 7 indicates that ΔF_r is proportional to the density and independent of the viscosity of the surrounding fluid. However, in the real QCM measurements, the surface roughness of the crystals, defined primarily by the manufacturing process, is not regular and deviates from the ideal cases as shown in Figure 1. Therefore, C_r should be viewed as a weak function of δ, in addition to being a function of the surface roughness.

3. Experimental Section

3.1. Chemicals and Crystals. Compressed helium (HP grade, 99.997%), nitrogen (UHP grade, 99.999%), and CO₂ (Coleman grade, 99.99%) were purchased from National Welders and used as received. Organic solvents of HPLC grade, ethanol, acetone, ethyl acetate, tetrahydrofuran, and trifluorotoluene, were obtained from Sigma-Aldrich. Water of extra high purity was obtained from Fisher Scientific.

The QCMs utilized consisted of silver or gold electrodes sputtered on both sides of a 5.00 MHz AT-cut quartz crystal. Three gold-sputtered and two silver-sputtered crystals were purchased from International Crystal Manufacturing (ICM), and the remaining silver-sputtered crystal (Ag-rough crystal) was obtained from Digi-Key Co. The crystals from ICM have a blank diameter of 8.5 mm, electrode diameter of 3.5 mm, and electrode thickness of 0.1 μm. The Digi-Key crystal has a blank diameter of 8.5 mm and electrode diameter of 6.00 mm. The three crystals of each type (silver or gold) were used as received; they were classified as polished (smooth), unpolished (slightly rough), or rough.

3.2. Pressure Cell and Apparatus. A schematic view of the pressure cell and the associated apparatus is provided in Figure 2. The custom-built pressure cell is a thick-walled cylinder (63.5 mm o.d., 17.5 mm i.d., and 150 mm long), with a high-pressure electrical feedthrough (Conax Buffalo Technologies, NY) at the top to drive the QCM. The cell has an internal volume of 25 cm³ and a maximum working pressure of 7500 psi. A thermocouple (Omega) is placed in the cell to indicate the temperature of the fluid. The pressure is monitored using a pressure transducer (Omega: DP-25-S-A) with 0.25% accuracy. The entire assembly is then placed in a water bath and controlled to 40 ± 0.1 or 35 ± 0.1 °C for all experiments.

N₂ or He is supplied to the pressure cell directly from an N₂ or He cylinder with a needle valve to control the addition of the

gas. In the case of CO_2, an ISCO 260D Series continuous flow syringe pump is connected after the CO_2 cylinder to supply CO_2 to the vessel. The fluid leaving the syringe pump or the cylinder flows through a valve, into a preheating coil immersed in the water bath, and finally into the cell.

During an experiment, the crystal is mounted in the cell and connected to an oscillator circuit through the electrical feed-through. The oscillator circuit is homemade and was adapted from that described by Melroy et al.[28] The oscillator circuit, powered by a triple output dc supply (BK Precision model 1651), is used to drive the crystal to vibrate. An Agilent 225 MHz Universal Frequency Counter (model 5313A) is connected to the circuit to read the frequency of the vibrating crystal. The time-dependent frequency readings are written to a computer by means of Agilent Ituilink Connectivity software.

3.3. Experimental Methods and Procedure of Frequency Determination. The surface roughness of the electrodes for each crystal was characterized using a Digital Instruments D3000 AFM with a Nanoscope III controller and extender module.

Each quartz crystal prior to the use was cleaned twice in water and a series of organic solvents ranging from polar to nonpolar, ethanol, ethyl acetate, acetone, tetrahydrofuran, and trifluoro-toluene. The crystal was placed for 5 min in each solution and was agitated.

A clean crystal was put into the pressure cell to determine the fundamental frequency, F_0, in a vacuum at a specific experimental temperature. The vacuum condition (at most 0.001 psi) was realized using a precision DD-20 model vacuum pump from VWR Scientific Products. The fundamental frequency (F_0) of the crystal was recorded after frequency stabilization in a vacuum for 20 min. The fluid was introduced into the cell at a given pressure, and the new values of the frequency, F_i, were continually recorded (every 5 s) until steady state had been reached. Steady state was defined as the point at which a change in frequency was observed to be less than ± 1 Hz over a long time scale (e.g., 10 min). Note that the full range of the frequency was 5 MHz; 1 Hz of frequency change was taken as the resolution of the QCM technique. The time to attain this condition was typically less than 25 min. The frequency shift at this pressure, ΔF_i, was calculated by subtracting F_0 from F_i. The fluid was then added again to the vessel to obtain a new pressure and new stabilized frequency. By this method, a series of ΔF values at elevated pressures (i.e., step experiments) for each crystal and each fluid (He, N_2, or CO_2) were obtained. Duplicate experiments for each run were done to obtain average ΔF values.

To calculate the frequency shift using the QCM theory, the densities of helium and nitrogen at different pressures were obtained from the NIST web database,[29] and the viscosities were calculated from equations described in the literature.[30,31] The densities and viscosities of CO_2 at different pressures were calculated using the CO_2Tab Property Add-in Software that was developed by ChemicaLogic Corp.[32]

4. Results and Discussion

Since the frequency of a QCM crystal exposed to a high-pressure fluid is simultaneously affected by different factors, it is critical to accurately separate out each influencing factor. Experimental verification of QCM theory enables the calculation of the actual mass change on the crystal surface. A unique strategy to verify the QCM theory in high-pressure fluids is to experimentally develop a relationship between the surface roughness of the crystal and frequency shift of the QCM. Therefore, atomic force microscopy (AFM) was used to characterize the surface roughness of six crystals (three gold and three silver crystals with different roughness), followed by three

(28) Melroy, O.; Kanazawa, K.; Gordon, J. G., II; Buttry, D. A. *Langmuir* **1986**, *2*, 697–700.

(29) http://webbook.nist.gov/chemistry/fluid/ (July 15, 2003).

(30) Najafi, B.; Ghayeb, Y.; Rainwater, J. C.; Alavi, S.; Snider, R. F. *Physica A* **1998**, *260* (1–2), 31–48.

(31) Stephan, K.; Krauss, R.; Laesecke, A. *J. Phys. Chem. Ref. Data* **1987**, *16* (4), 993–1023.

(32) http://www.chemicalogic.com/co2tab/default.htm (July 15, 2003).
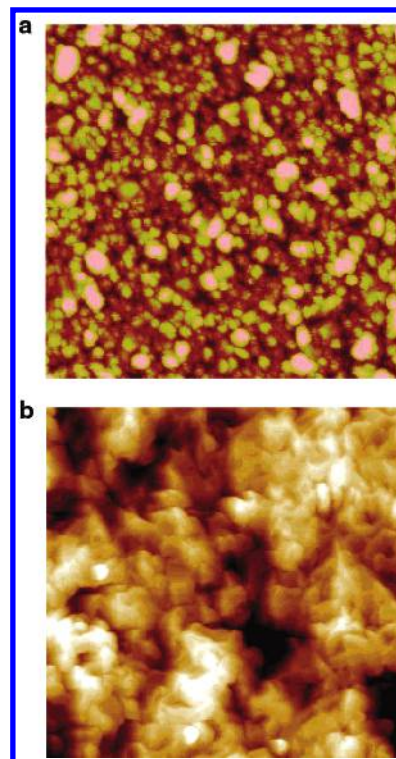
Figure 3. AFM images of two silver-sputtered QCM crystals. (a) Ag-polished crystal (3×3 μm^2 with Z range of 15 nm); (b) Ag-rough crystal (75×75 μm^2 with Z range of 3.88 μm).

groups of QCM experiments. The first set of experiments were performed on Ag-polished (40 °C) and Ag-rough crystals (35 °C) utilizing He, the lightest and nonabsorbing inert gas, to determine the pressure and viscosity dependence of frequency, ΔF_P and ΔF_η. To evaluate the roughness contribution to the frequency, ΔF_r, the second set of experiments was performed for all six crystals utilized N_2, another nonabsorbing gas on the metal surfaces at 35 or 40 °C. The last group of experiments for all six crystals was conducted on low-density gaseous CO_2 (<0.2 g cm^{-3}) at 35 or 40 °C, an adsorbing gas, to test the adsorbed mass of CO_2 on metal surfaces (silver or gold). Finally, the adsorption of supercritical CO_2 on metal surfaces at 40 °C was determined using the reformulated QCM calculation approach.

4.1. Characterization of the Crystal Surface. As described in the QCM theory, the microscopic properties of the crystal–fluid interface affect the measured QCM frequency. The most important features of the crystal–fluid interface were characterized using the AFM technique. These characterization parameters were the root-mean-square (rms) roughness, the ratio of three-dimensional surface area to its projected area (R_a), the average height (h) and lateral length (a) of periodic inhomogeneities, and the average distance (l) between inhomogeneities. The rms roughness is defined as the root-mean-square (or standard deviation) of all Z_i values within a given AFM image area with respect to the average value of all Z_i data, Z_{ave}, where Z_i is the vertical distance of a point on the rough surface to a preset (X, Y) plane. The three-dimensional surface area is the sum of the area of all of the triangles formed by every three adjacent data points on the surface, which is characteristic of the actual surface area. The remaining parameters, h, a, and l, have been defined in Figure 1.

AFM images of two silver-sputtered crystals are shown in Figure 3 as examples, and the aforementioned parameters are summarized in Table 1. The rms roughness

Table 1. Some Characteristic Properties of Six Different Crystals

crystals	rms roughness (10^{-7} cm)	$R_a{}^a$	h (10^{-7} cm)	a (10^{-7} cm)	l (10^{-7} cm)	C_r (10^{-5} cm)^c		
						eq 8a	eq 8b	eq 8c
Ag-polished	3.7	1.02	12	180	190	1.00	$1.32(1-2.65\rho_f)$	$0.398 + 4.96 \times 10^4\delta$
Ag-unpolished	26	1.04	85	1410	2180	1.25	$1.79(1-3.48\rho_f)$	$0.322 + 7.44 \times 10^4\delta$
Ag-rough^{b,d}	647	1.08	1030	n.a.	n.a.	6.43	$7.28(1-1.27\rho_f)$	$5.16 + 1.05 \times 10^5\delta$
Au-polished	2.8	1.02	8	110	120	1.10	$1.37(1-2.23\rho_f)$	$0.595 + 4.10 \times 10^4\delta$
Au-unpolished	115	1.19	210	1370	2120	2.54	$3.22(1-2.37\rho_f)$	$1.41 + 9.17 \times 10^4\delta$
Au-rough^{b,d}	681	1.15	1090	n.a.	n.a.	6.04	$6.88(1-1.51\rho_f)$	$3.99 + 1.63 \times 10^5\delta$

^{a} R_a is the ratio of three-dimensional surface area to its projected area. ^{b} Data were collected with low-resolution AFM (75×75 μm^2) due to large feature sizes. ^{c} The units for ρ_f and δ are g cm^{-3} and cm, respectively. ^{d} Lack of data due to the difficulty of evaluating a and l for strongly rough crystals.
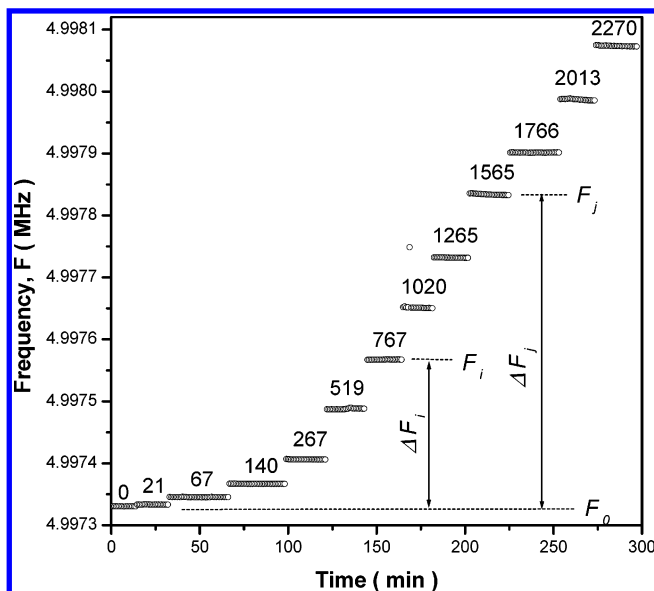
Figure 4. A typical run in helium for the determination of time-dependent QCM frequency data at elevated pressures (numeral data, psi). The calculation of frequency shift, ΔF_i or ΔF_j, at each pressure is also shown.

Figure 5. Plots of frequency shift versus pressure measured at 40 °C on Ag-polished (■, N₂; ▼, He), Ag-unpolished (●, N₂), Ag-rough (▲, N₂; ▽, He at 35 °C), Au-polished (□, N₂), Au-unpolished (○, N₂), and Au-rough (△, N₂) crystals. The insert shows the frequency responses at low pressures, and the dashed line represents eq 3.

ranged from several nanometers (polished crystals) to several hundred nanometers (rough crystals) for either silver or gold crystals. The values of both a and l varied from several hundred nanometers to several micrometers. The average height, h, was found to be almost twice the rms roughness. The polished and unpolished crystals had periodic inhomogeneities (see Figure 3a), from which the parameters of a and l were obtained. For the rough crystals, since no apparent periodic inhomogeneities were found in the AFM images (see Figure 3b), it was difficult to obtain the values of a and l. In addition, due to the large roughness of these crystals, the AFM images were taken with a larger scale of dimension (75×75 μm^2). This lower resolution led to the underestimation of the three-dimensional area, which influenced the accuracy of R_a. In this case, except for the R_a data, other parameters were good representatives of the surface roughness.

4.2. Separation of Factors Influencing QCM Frequency. Figure 4 demonstrates a typical run for the determination of time-dependent QCM frequency data at elevated pressures. Steady state frequency at each pressure was obtained in 25 min, and the frequency shift (ΔF_i) was calculated as shown in the same figure. It was found that the determined frequency shifts between two parallel experiments deviated less than 4 Hz for all the data presented in this paper. This gave an average relative deviation of $\pm 2\%$ for large ΔF_i data (absolute value > 50 Hz) and a deviation of about $\pm 5\%$ for small ΔF_i data (<20 Hz).

The frequency shifts of all six crystals in nitrogen and those of two silver-sputtered crystals in helium were determined at elevated pressures and are shown in Figure 5. In nitrogen systems, the ΔF decreased at low pressures and underwent a minimum for all six crystals. The minimum ΔF was located at a pressure ranging from 20 to 200 psi and decreased with increasing roughness of the crystals. After the minimum, the ΔF increased almost linearly with increasing pressure and decreased with increasing roughness at each pressure. In the case of helium systems, the ΔF increased linearly with increasing pressure and was always lower than ΔF_P, the theoretical pressure contribution to frequency based on eq 3 (Figure 5). Such phenomena in nitrogen and helium were similar to the observations made by Tsionsky et al. on gold- and nickel-sputtered crystals.[22] However, our experiments were performed over a wider range of pressure (1800 versus 750 psi).

Theoretical calculations were performed and compared with the experiments. In the calculations, $\Delta F_m = 0$ was assumed for the helium systems since helium is the lightest, nonabsorbing, inert gas. For the nitrogen systems, a molecular monolayer of N₂ on a real surface was reported to be 6×10^{14} molecules per cm^2 by Young and Crowell,[33] which corresponds to 28 ng cm^{-2}. This mass of N₂

(33) Young, D. M.; Crowell, A. D. *Physical adsorption of gases*; Butterworth: London, 1962.

corresponds to a frequency shift (ΔF_m) of -3.2 Hz according to eq 2. Hence, the monolayer adsorption of N_2 on metal surfaces was assumed, and $\Delta F_\text{m} = -3.2$ Hz for all the pressure conditions. The calculations showed that the total frequency shift (ΔF) of a QCM crystal in helium was contributed primarily from the pressure and viscosity effects (ΔF_P and ΔF_η). For the Ag-polished crystal in helium, using eqs 3 and 4 to calculate the theoretical ΔF led to a prediction of 104% of the experimental ΔF, and the roughness contribution of frequency, ΔF_r, was negligibly small. However, for the Ag-rough crystal in helium, the experimental frequency shift was about 15% lower than the sum of the theoretical ΔF_P and ΔF_η, which had to be attributed to the roughness effect. For the same reason, for all six crystals in N_2, the total frequency shift was greatly affected by the roughness contribution.

To isolate ΔF_r from other factors, the experimental roughness contribution in N_2, $\Delta F_\text{r(exp)}$, was calculated by subtracting theoretical ΔF_m, ΔF_P, and ΔF_η from the experimental ΔF. The resulting $\Delta F_\text{r(exp)}$ in N_2 was plotted as a function of N_2 density. The frequency shift corrected in this manner was found to be almost a linear function of density. Comparing $\Delta F_\text{r(exp)}$ with the theoretical ΔF_r of eq 7, the frequency–roughness correlation factor, C_r, can be calculated using eqs 8a–c:

$$C_\text{r} = a_0 \tag{8a}$$

$$C_\text{r} = a_1(1 + b_1\rho_\text{f}) \tag{8b}$$

$$C_\text{r} = a_2 + b_2\delta \tag{8c}$$

where a and b are the constants assumed to be independent of the type of fluid. The values of a and b for each crystal were summarized in Table 1. As could be seen, C_r was primarily a strong function of rms roughness (or h) and secondarily dependent on a and l. C_r increased with the rms roughness slowly at low rms values ($<26 \times 10^{-7}$ cm) and rapidly at high values. The parameters a and l affected C_r indirectly by varying the roughness profile (h/l and h/a).

Equation 8a was a good approximation for the polished and rough crystals, with correlation coefficients of 0.99. However, the correlation coefficients were poor (<0.98) for the unpolished crystals. This might be due to the insufficiency in satisfying the conditions of $a/\delta \gg 1$ and $a/\delta \ll 1$ for the unpolished crystals that had moderate roughness. In this work, eq 8a was applicable to low-density gases (<0.1 g cm^{-3}) and should be used as a rough estimation of C_r. Equation 8b, a first-order density approximation, represented an accurate prediction of C_r for all six crystals with correlation coefficients better than 0.997. This equation could be applied to gases (<0.2 g cm^{-3}) with high accuracy but was not suitable for liquids. This was because the viscosity effect was not accounted for. The viscosities between the gases are very similar, but they differ largely between gases and liquids. To fully account for the density and viscosity dependence of C_r, eq 8c, a first-order decay length approximation, could be used to replace eq 8b. The linearity between C_r and δ was well established with correlation coefficients better than 0.997, when the δ values were lower than 2×10^{-5} cm. Therefore, eq 8c was believed to be applicable for fluids (e.g., gases, supercritical CO_2, and liquids) of similar δ range.

Equation 8b obtained from N_2 systems was used to calculate C_r, and the total ΔF in helium ($=\Delta F_\text{P} + \Delta F_\eta + \Delta F_\text{r}$) was repredicted by including the roughness contribution. The predicted ΔF was 102% of the experimental
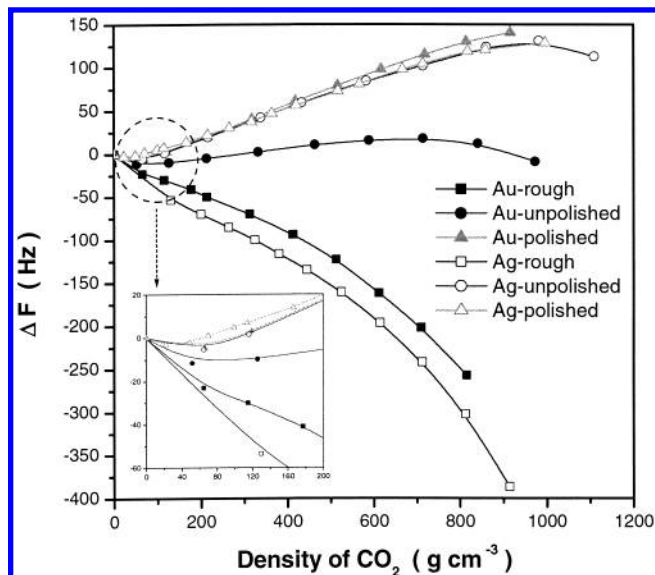
Figure 6. Plots of frequency shift in gaseous CO_2 versus density at 35 °C for the Ag-rough crystal and at 40 °C for all remaining crystals. The insert shows the frequency responses at low densities.

value for both crystals in helium, indicating the accuracy of the QCM theory and the independence of C_r on the fluid type.

4.3. Adsorption of Gaseous CO_2 on Metal Surfaces: Examination of QCM Theory. The frequency changes of all six crystals in gaseous CO_2 were measured and are shown in Figure 6. It was found that at each pressure the experimental values always had the following order of decreasing ΔF: polished > unpolished > rough for both silver and gold crystals. The ΔF value decreased at low pressures, underwent a minimum, and then increased almost linearly with increasing pressure for the four crystals that have small rms roughness values. It behaved similarly as in the case of N_2 systems. However, for the remaining two crystals that have large rms values (i.e., Ag-rough and Au-rough), ΔF decreased with increasing pressure of gaseous CO_2.

The adsorption amounts, Δm, of gaseous CO_2 on silver and gold surfaces were calculated from ΔF_m using eq 2. ΔF_m was found by subtracting the theoretical ΔF_P (eq 3), ΔF_η (eq 4), and ΔF_r (eqs 7 and 8b) from experimental ΔF. In the calculation of frequency–roughness correlation factors, C_r, in eq 8b, the CO_2 density was used to replace the N_2 density, while the constants of a_2 and b_2 were kept the same.

The calculated adsorption amounts of CO_2 on three gold and three silver surfaces as a function of the CO_2 density, as well as the average values of CO_2 adsorption (solid line), are shown in Figure 7. As can be seen, all six crystals having different roughness values and electrode materials (silver or gold) adsorbed similar amounts of gaseous CO_2 per real surface area, and the CO_2 adsorption increased with increasing CO_2 density. The average deviation of CO_2 adsorption for each crystal from the average value at each pressure was only about 0.05 μg cm^{-2}. Based on one molecule of CO_2 occupying an area[33] of 17×10^{-16} cm^2, the mass of 0.05 μg cm^{-2} corresponds to one full monolayer of CO_2 molecules on the real surface that resulted in a 6 Hz change in frequency. This 6 Hz change in frequency was negligible and close to experimental error (±2 Hz). Besides the experimental error, this deviation might also be incurred by the correlation accuracy of C_r in eq 8b. An example of this type of deviation was the CO_2 adsorption
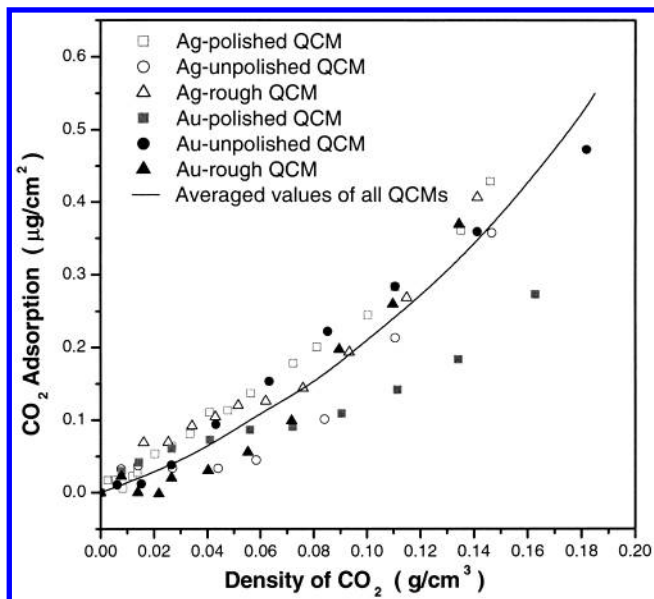
Figure 7. Plots of adsorption of gaseous CO_2 on silver and gold surfaces as a function of CO_2 density. In the calculation, the C_r values were obtained from eq 8b.

Figure 8. Frequency shift of Ag-polished and Ag-rough crystals in gaseous and supercritical CO_2 at 40 °C as a function of pressure.

on Ag-unpolished crystal. In this case, the correlation coefficient (0.997) of C_r had the lowest value of all three silver-sputtered crystals (>0.999 for the other two), leading to smaller CO_2 adsorbed amounts than the average values. For the Au-polished crystal, when the CO_2 density was larger than 0.09 g cm⁻³, large deviations (>0.05 μg cm⁻²) of CO_2 adsorbed amounts from the average values were found. This could be attributed to the adsorbed CO_2 layers that could fill up some small holes or valleys on the crystal surface. Since the Au-polished crystal had the smallest rms roughness (2.8 nm) and a faster varying surface (smaller a and l) as compared to the other crystals, a small modification of the surface by the absorbed CO_2 layers could diminish the surface roughness and thus cause a decrease in C_r.

Theoretically, no matter how different the surfaces were, the CO_2 adsorption per unit real surface area should have been the same for the same material. The fact that the experimentally calculated CO_2 adsorption (or condensation) was very close for each type of crystal surface led to additional evidence of the exactness of the reformulated QCM theoretical approach as presented in eqs 7 and 8. It also implied that the a and b values obtained from N₂ experiments are independent of the type of fluid in contact with QCM crystals. In addition, the CO_2 adsorption on silver or gold surfaces ranged up to 0.5 μg cm⁻² at the CO_2 density of 0.18 g cm⁻³. This amount of adsorbed or condensed CO_2 corresponded to 10 full molecular layers, assuming a flat configuration for the surface.

4.4. Adsorption of Supercritical CO₂ on Metal Surfaces. The frequency response of Ag-polished and Ag-rough crystals in CO_2 at 40 °C and elevated pressures up to 3200 psi is presented in Figure 8. For the Ag-polished crystal, the frequency behavior at low pressures (<900 psi) was described in section 4.3. At high pressures, the frequency shift continued to increase over the entire pressure range except in the vicinity of the critical pressure, where the value decreased rapidly until it leveled out at 1450 psi. As for the rough crystal, the frequency response was similar to that of the polished crystal; however there was a large depression in frequency around the critical pressure.
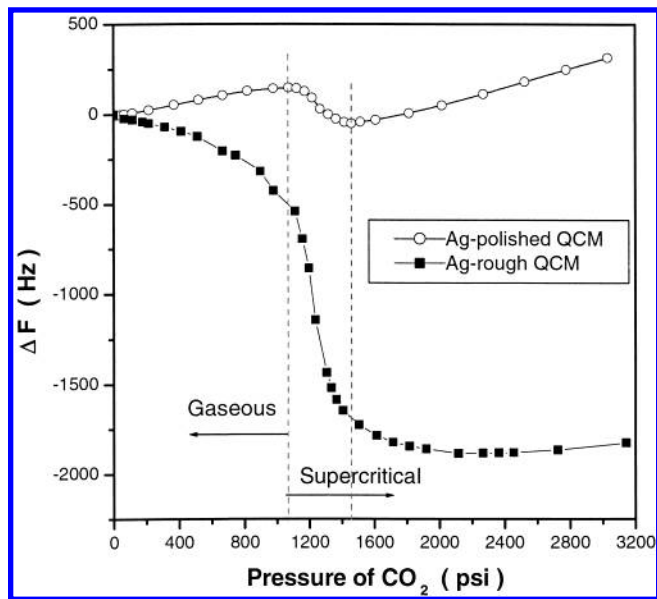
The adsorption/condensation of CO_2 over the experimental range of densities is presented in Figure 9. The calculation procedure was the same used for gaseous CO_2. Since the δ for CO_2 at 40 °C ranges from 1.8 to 0.7 × 10⁻⁵ cm when the CO_2 density is larger than 0.03 g cm⁻³, eq 8c is the most applicable to calculate the roughness contribution to the frequency shift. However, the results shown in Figure 9a indicate that the calculated CO_2 adsorption at higher densities (>0.4 g cm⁻³) decreased with increasing density for both crystals. In particular, the experimentally determined CO_2 adsorption at higher densities became negative for the Ag-rough crystal. Analysis has shown that as the CO_2 density and the amount of adsorbed CO_2 increase, the holes and valleys between the inhomogeneities on the crystal surface are gradually filled (see inset, Figure 9b), which causes a gradual decrease in surface roughness value and then in C_r. Urbakh and Daikhin[14] theoretically analyzed and demonstrated that adsorbed layers of a substance could modify the surface roughness and then affect the surface roughness contribution to the frequency. Therefore, in this case, C_r should be corrected for the overestimation of the roughness contribution; we proposed the following equation to accomplish this:

$$C_r = (a_2 + b_2\delta)\xi/\xi_0 \qquad (8d)$$

where ξ_0 and ξ are the roughness (i.e., the rms roughness) of the original real surface and the modified surface by the absorbed molecules, respectively. If the CO_2 adsorption is assumed to be small, ξ is a function of ξ_0 and the thickness or mass, Δm, of absorbed molecular layers. However, when the adsorption is large, since the absorbed molecules fill and level up the small holes and valleys first, followed by the larger features, ξ is additionally dependent on the distributions of surface roughness features, not merely an average value of the roughness. Since the CO_2 absorption or condensation increased with increasing density and was larger than 10 molecular layers at densities larger than 0.2 g cm⁻³ (see section 4.3), the determination of CO_2 adsorption under supercritical conditions using rough QCM crystals became complicated.

Interestingly, it was found that the CO_2 adsorption under supercritical conditions could still be accurately
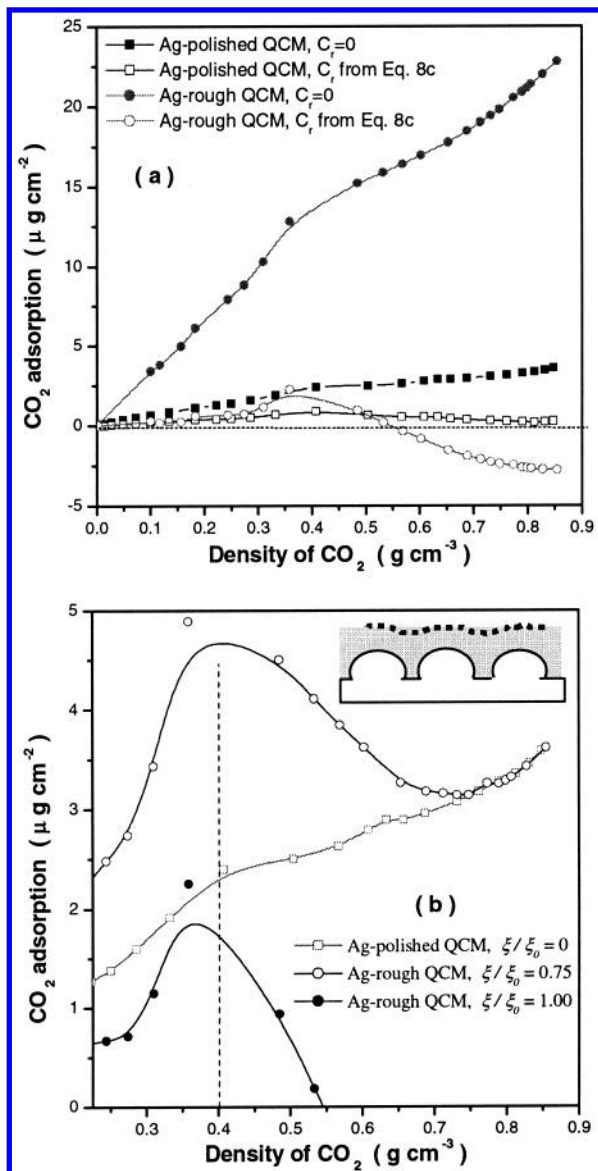
Figure 9. Comparison of different calculation methods for the adsorption of CO_2 on silver surfaces from the frequency data of Ag-polished and Ag-rough crystals. (a) CO_2 adsorption in the entire density range with and without the consideration of the roughness contribution to the frequency; (b) adsorption of supercritical CO_2 after correcting the overestimation of surface roughness. The inset in panel b illustrates how adsorbed mass of CO_2 modifies the surface roughness.

determined using the Ag-polished crystal. As shown in Table 1, the average width (or diameter) for the holes or valleys ($w = l - a$) on the polished crystal surface was about 10 nm, while the average depth was 12 nm (approximately equal to h). This scale of dimension is equal to 20−25 layers of CO_2 molecules or, equivalently, about 1−1.2 μg CO_2 mass adsorbed per cm^2 of real area. Since the wall of a hole is a closed loop and also adsorbs CO_2, 1.2 μg CO_2 mass per cm^2 can fill all the holes or valleys that have a depth of $\leq h$ or a diameter of $\leq 2w$. Even though the distributions of the depth and diameter of holes were unknown, by assuming Gaussian distributions, the largest feature on the surface has a depth of $2h$ and a diameter of $2w$. This dimension of the largest feature can be completely smoothed by 2.4 μg CO_2 mass adsorbed per cm^2 of surface area. Therefore, it was deemed that the calculation of adsorption of supercritical CO_2 using $C_r = 0$ (or $\xi = 0$), when the CO_2 density is larger than 0.4 g

cm^{-3}, was appropriate. In this case, the adsorption (open squares in Figure 9b) of supercritical CO_2 ranged from 2.4 to 3.6 μg cm^{-2} when the CO_2 densities were changed from 0.4 to 0.85 g cm^{-3}. Also, since the adsorption of gaseous CO_2 on silver surfaces was nearly the same as that on gold surfaces (section 4.3), it was believed that the adsorption of supercritical CO_2 on the gold surface was also similar to that on the silver surface. Moreover, assuming $C_r = 0$ may not be accurate when calculating the adsorption amount in the presence of supercritical or gaseous CO_2 within a density range of 0.18−0.4 g cm^{-3}.

The adsorption in the presence of supercritical CO_2 on the Ag-rough crystal was recalculated and is shown in Figure 9b, by imposing a limit for ξ/ξ_0 to be between 0.75 and 1.00. As determined in the current study, when the CO_2 density is lower than 0.4 g cm^{-3}, the calculated amounts of supercritical CO_2 adsorption (solid circles in Figure 9b) using $\xi/\xi_0 = 1.0$ were close to the values obtained from the Ag-polished crystal (open squares in Figure 9b). When the CO_2 density changed from 0.72 to 0.85 g cm^{-3}, the calculated adsorption using $\xi/\xi_0 = 0.75$ was nearly the same for the Ag-polished crystal (open circles in Figure 9b). In the density range of 0.4−0.72 g cm^{-3}, ξ/ξ_0 changed gradually from 1 to 0.75. This comparison provided additional evidence that the adsorption/condensation of supercritical CO_2 obtained on the Ag-polished crystal was accurate when the CO_2 density is larger than 0.4 g cm^{-3}.

In the literature, Otake et al.[16] and Guigard et al.[17] determined the mass of supercritical CO_2 adsorbed onto rough silver and gold QCM electrodes at 40 °C, respectively. They concluded that the adsorption on silver and gold surfaces could go up to 25 μg cm^{-2}, which agrees well with the calculation for the Ag-rough crystal using $C_r = 0$ (solid circles in Figure 9a). However, we have shown in this study that to fully elucidate the frequency response in CO_2 the surface roughness effect must be accounted for. In addition, this work has shown that in order to obtain accurate data of adsorption of supercritical CO_2 on a rough surface it was crucial to estimate the variation of C_r with adsorbed molecular layers.

5. Conclusions

The successful use of the QCM technique in high-pressure fluids, especially supercritical CO_2, relies on the experimental examination of the QCM theory utilized for the calculation of mass change on a surface. To separate out all factors influencing frequency, the frequency responses of six QCM crystals with different electrode materials (silver or gold) and roughness values were determined in helium, nitrogen, and carbon dioxide at 35−40 °C and at pressures up to 3200 psi. It was revealed that the role of surface roughness on the frequency response of a crystal in contact with adsorbing and nonadsorbing fluids is critical to validate the QCM theory at high pressure. A new calculation approach was developed to include the roughness contribution to the frequency. It was found that the frequency−roughness correlation factor, C_r, in the new approach was a characteristic measure of roughness and enabled the accurate calculation of the roughness contribution to the frequency.

At low CO_2 densities and low amounts of adsorption or condensation, all six crystals absorbed similar amounts of gaseous CO_2, irrespective of the roughness and type of the electrodes. This implies the applicability of the reformulated QCM calculation approach in this work. The extension of this approach to other conventional systems (i.e., liquids) is straightforward. However, when the CO_2 density and the amount of CO_2 adsorbed were higher, the

use of moderate to very rough QCM crystals (tens to several hundreds of nanometers) required careful attention due to the variation of C_r. Only very smooth QCM crystals (several nanometers or less) are capable of accurately determining the adsorption of supercritical CO_2 on the metal surfaces without adjusting the frequency shift to account for roughness issues. When CO_2 densities were less than 0.85 g cm^{-3}, the adsorption/condensation of gaseous and supercritical CO_2 onto the silver and gold surfaces ranged to 3.6 μg cm^{-2} at 40 °C, but not up to 25 μg cm^{-2} as determined by Otake et al. and Guigard et al. who used very rough crystals and neglected the roughness contribution. This study provided theoretical fundamentals for the successful use and future work of the QCM technique in high-pressure CO_2, as well as in other conventional systems. Current research is underway to utilize the micro-weighing capability of the QCM to evaluate the kinetics and the dissolution behavior of polymer films under supercritical conditions.

LA035502F